Sensors & Actuators: B. Chemical 273 (2018) 1456–1462

Contents lists available at ScienceDirect

Sensors and Actuators B: Chemical

journal homepage: www.elsevier.com/locate/snb

An ultrasensitive fluorescence sensing strategy for detection and *in situ* imaging of chronic myeloid leukemia-related BCR-ABL1 mRNA

Xiao-yan Zhou[a,1], Jian-hua Pan[a,1], Yong-neng Ma[c,1], Xiu-juan Peng[c], Hai-ping Wu[a], Qin Zhou[a], Shi-jia Ding[a,*], Huang-xian Ju[a,b,**]

[a] Key Laboratory of Clinical Laboratory Diagnostics (Ministry of Education), College of Laboratory Medicine, Chongqing Medical University, Chongqing 400016, China
[b] State Key Laboratory of Analytical Chemistry for Life Science, School of Chemistry and Chemical Engineering, Nanjing University, Nanjing 210023, China
[c] Department of Clinical Laboratory, Third People's Hospital of Mianyang country, Sichuan 621000, China

ARTICLE INFO

Keywords:
Isothermal amplification
Fluorescence
Biosensing
Chronic myeloid leukemia
BCR-ABL1 mRNA

ABSTRACT

In this study, a fluorescent sensing strategy has been developed for rapid and ultrasensitive detection of BCR-ABL1 mRNA in chronic myeloid leukemia (CML) based on DNAzyme Cleavage-induced Rolling circle amplification (DCR for short). In the presence of BCR-ABL1 mRNA, DNAzyme was activated to split the target sequence into two fragments, producing the 3′ terminus on the forward cleavage fragments. After T4 polynucleotide kinase (PNK) modification reaction, the forward cleavage fragments were extended by rolling circle amplification (RCA). Plenty of long single DNA strands were produced and partially hybridized with the fluorescence-quenching decorator probes, thus inducing the separation of fluorophore and quencher decorator probes and recovery of fluorescence. Highly sensitive detection of BCR-ABL1 was achieved with a limit of detection at 9.4 fM. In addition, the DCR strategy was adopted to successfully *in situ* image the BCR-ABL1 mRNA in the cytoplasm of human leukemia bone marrow cells. Moreover, results of the BCR-ABL1 mRNA expression in clinical samples achieved by DCR sensing were well consistent with that of reverse transcription PCR (RT-PCR) and fluorescence *in situ* hybridization (FISH) analysis. Therefore, this developed DCR sensing strategy might provide a potential alternative tool for precise diagnosis of CML.

1. Introduction

Chronic myeloid leukemia (CML) is a clonal myeloproliferative disease with the cytogenetic hallmark of Philadelphia chromosome (Ph) [1]. The Ph is generated by the reciprocal translocation between the long arms of chromosomes 9 (ch9) and 22 (ch22), resulting the creation of the BCR-ABL1 fusion gene and the transcription of BCR-ABL1 mRNA [2]. Previous reports demonstrate the BCR-ABL1 transcript plays a significant role in the pathogenesis of leukemogenesis [3], and causes the feared blast crisis in CML by inducing the suppression of cell apoptosis [4]. Hence, the development of approaches for measuring BCR-ABL1 mRNA has great significance for precise diagnosis and treatment of CML.

Currently, a variety of techniques have been applied to measure BCR-ABL1, such as fluorescence *in situ* hybridization (FISH) [5] and quantitative real-time reverse-transcription polymerase chain reaction (qRT-PCR) [6]. FISH can visualize BCR-ABL1 in cytoplasm by fluorescent dye-labeled probe hybridization in the fusion site, but typically with lower analytical sensitivity. RT-PCR is used to rapidly amplify BCR-ABL1 mRNA, but the complicated pretreatment of RNA by cDNA synthesis can cause cross-contamination with genomic DNA and increase the probability of false positive [7,8]. Additionally, the RT-PCR technique relies on thermal cycling, limiting the technique to a laboratory setting. Therefore, to overcome these drawbacks, the exploration of novel methodology for detecting the mRNA expression of BCR-ABL1 is highly desirable.

So far, there is growing interest in the development of isothermal amplification-based biosensing strategies for simple and efficient detection of nucleic acid, such as rolling circle amplification (RCA) [9,10], strand displacement amplification (SDA) [11], catalytic hairpin assembly (CHA) [12] and loop-mediated isothermal amplification (LAMP) [13]. As one of the most fascinating isothermal amplification

* Corresponding author.
** Corresponding author at: Key Laboratory of Clinical Laboratory Diagnostics (Ministry of Education), College of Laboratory Medicine, Chongqing Medical University, Chongqing 400016, China.
E-mail addresses: dingshijia@cqmu.edu.cn, dingshijia@163.com (S.-j. Ding), hxju@nju.edu.cn (H.-x. Ju).
[1] These authors contributed equally to this work.

https://doi.org/10.1016/j.snb.2018.07.032
Received 29 March 2018; Received in revised form 3 July 2018; Accepted 6 July 2018
Available online 07 July 2018

technique, RCA has been shown to detect nucleic acids with a variety of outstanding properties, including simple operation and highly amplified efficiency [14,15]. It has been acknowledged that DNA and microRNA could be detected based on RCA sensing strategy with improved sensitivity of 3–6 orders of magnitude over conventional methods [16–18]. Additionally, RCA is utilized not only in detecting nucleic acids of extracts from cancerous cells [19], but also in visualizing the intracellular nucleic acids [20,21]. For instance, some groups used the target RNA as a template to ligate a padlock probe *in situ*, which successfully realized *in situ* amplification of RNA [22–24]. However, extra short DNA strands need to be added in the reaction as a primer in the above methods, increasing the non-specific amplification during RCA process. Nevertheless, RCA is a versatile tool to detect nucleic acids with the remarkable capacity for rapid analysis, significant amplification efficiency and operational simplicity.

Deoxyribozymes (DNAzymes) have attracted widespread attention for their efficient catalytic activity, high chemical stability, simple synthesis, and easy modification [25–27]. RNA-cleaving DNAzyme is the widely investigated class of DNAzymes [28], including the 10–23 DNAzyme [29,30] and 8–17 DNAzyme [31,32]. 10–23 DNAzyme contains a 15-nucleotide catalyze core and two substrate-recognition domains, which can cleave any purine-pyrimidine (R–Y) junction under metal ions condition [33]. Owing to the highly specific substrate recognition and cleavage of DNAzyme, a series of DNAzyme feedback amplification strategies have been constructed for sensitive detection of microRNA and bacterium [17,34,35]. More importantly, many researchers have used DNAzyme to cleave BCR-ABL related mRNA in cells for potential treatment of CML [36,37]. Inspired by these advantages of functional DNAzyme, the utilization of DNAzyme to efficiently detect the BCR-ABL1 mRNA level will have a significant application prospect.

In this work, a fluorescence sensing strategy termed DNAzyme Cleavage-induced RCA (DCR for short) is constructed for rapid amplification and ultrasensitive detection of BCR-ABL1 mRNA. As illustrate in Scheme 1A, two recognition domains on the flank of DNAzyme are designed to specifically recognize and hybridize with BCR-ABL1 mRNA sequence. The DCR sensing strategy contains three reactions (Scheme 1B), including (i) DNAzyme cleavage, (ii) T4 polynucleotide kinase (PNK) modification, and (iii) the RCA process. In cleavage reaction, upon the introduction of RNA target, the DNAzyme-RNA complex is formed. In the presence of Mg^{2+}, the RNA is cleaved into two fragments (f1 with a 2′, 3′-cyclic phosphate terminus and f2 with a 5′-hydroxyl terminus) by DNAzyme. DNAzyme separated from the complex takes part in another cycle of cleavage reaction, and the forward-cleaved f1 participates in the subsequent reactions. In the modification reaction, the 2′, 3′ cyclic phosphate terminus of f1 is removed by T4 PNK to yield a hydroxy terminus on the f1′, which can act as a primer to trigger the RCA process. Meanwhile, the closed circular DNA template is introduced into the cleavage products, which strand displacement take place of DNAzyme to hybridize with primer f1′. During the RCA process, plenty of long single DNA strands is produced and partially hybridize with the fluorescence-quenching decorator probes, thus inducing the separation of fluorophore and quencher. Finally, the fluorescence signals are successfully achieved, which is highly related to the concentration of the analyte. With adoption of DCR sensing strategy, BCR-ABL1 mRNA expression can be assayed without RNA purification, cDNA synthesis or thermal cycling. Moreover, the BCR-ABL1 mRNA could be accurately visualized in the cytoplasm of human leukemia cells.

2. Material and methods

2.1. Materials and reagents

Phi29 DNA polymerase, T4 polynucleotide kinase (PNK), and RNase inhibitor were purchased from New England Biolabs (Beijing, China). T4 DNA ligase, exonuclease I, exonuclease III, dsDNA marker and DNA fragment purification kit were purchased from TaKaRa (Dalian, China). Tween-20, Triton X-100, 4′, 6-diamidino-2-phenylindole (DAPI), 4% paraformaldehyde fix solution, anti-fade mounting medium, dNTPs and all other chemicals were of analytical reagent grade and purchased from Sangon Biotechnology Co. Ltd (Shanghai, China) and used without further purification. All solutions were prepared with ultrapure water by Millipore Milli-Q gradient ultrapure water system (Millipore, MA).

All sequences of oligonucleotides used in this work were listed in Tables S1 - S3 [36]. All DNA and RNA sequences were purchased from Sangon Biotechnology Co. Ltd (Shanghai, China) and TaKaRa (Dalian, China), respectively. The decorator probe components were yielded by heating the mixture of 3′-fluorophore-labeled D-oligo and 5′-BHQ1-labeled C-oligo with a ratio of 1:2 (ensure complete quenching of the fluorescence) to 95 °C for 5 min, then cooled to room temperature for 2 h.

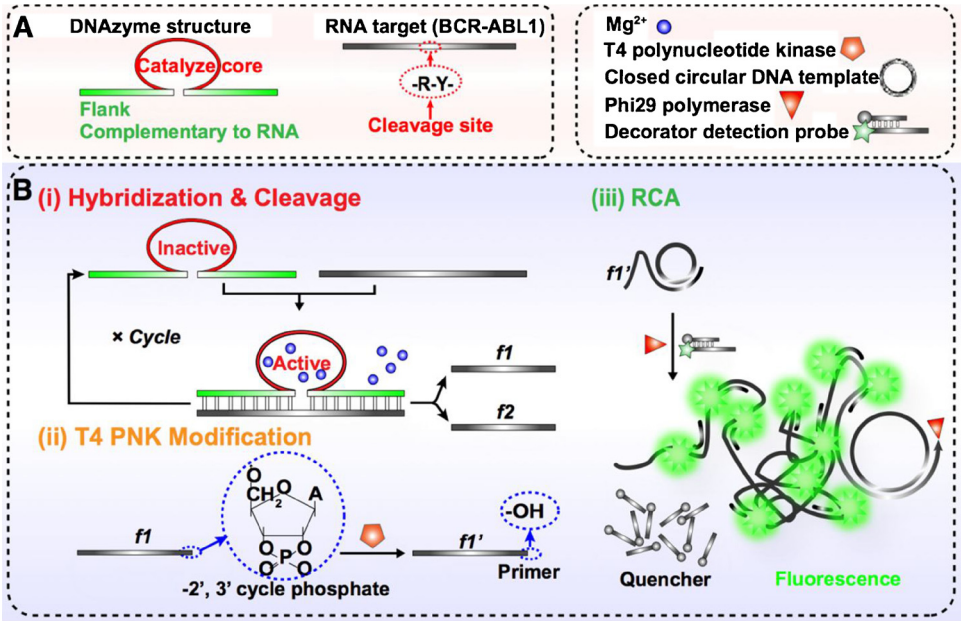

Scheme 1. Principle of DNAzyme cleavage-induced RCA (DCR) for BCR-ABL1 mRNA detection. (A) The structure of DNAzyme and the 'R-Y' cleavage site in RNA target of BCR-ABL1. (B) (i) Site-specific cleavage of RNA target by DNAzyme in the presence of Mg^{2+}; (ii) Removal of the 2′, 3′ cyclic phosphate terminus of forward cleavage fragment (f1) by T4 PNK; (iii) RCA process and fluorescence detection of the RCA products.

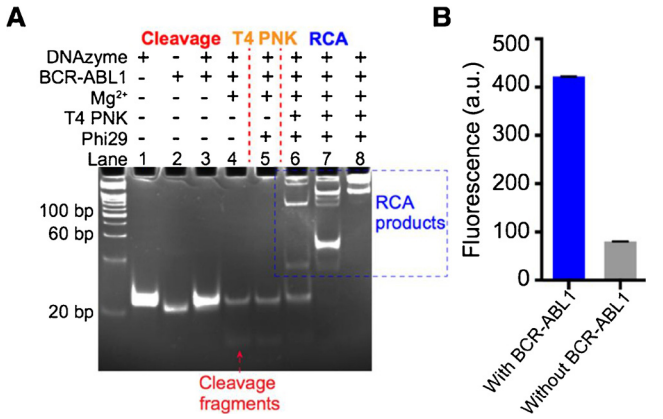

Fig. 1. Examination of DCR for BCR-ABL1 RNA detection. (A) Native PAGE results for the different reactions. Lane 1: DNAzyme; lane 2: BCR-ABL1; lane 3: DNAzyme (1 μM) and BCR-ABL1 (500 nM); lane 4: BCR-ABL1 cleaved by DNAzyme with Mg^{2+} (50 mM). The cleavage fragments have slightly faster mobility; lane 5: No amplification of the closed circular DNA template (200 nM) by Phi29 polymerase (0.5 U/μL) without T4 PNK; lanes 6–8: After T4 PNK treatment, amplification of the closed circular DNA template by Phi29 polymerase with different RCA time (lane 6, 15 min; lane 7, 30 min; lane 8, 60 min). (B) Fluorescence spectra of DCR sensing with or without BCR-ABL1 RNA target (100 nM).

2.2. Patient samples

A total of 12 extracted total RNA samples and 12 bone marrow (BM) cell samples from patients with BCR-ABL1 positive leukemia were obtained from the First Affiliated Hospital of Chongqing Medical University, with approval by the ethical committee of the hospital for only laboratory study.

2.3. Pretreatment of total RNA and BM cell

Total RNA was extracted from peripheral blood using high purity UNIQ-10 RNA isolation kit (Sangon Biotechnology Co. Ltd) according to the manufacturer's instructions. The RNA concentration was measured using the NanoDrop 2000 (Thermo Scientific). Complementary DNA (cDNA) was transcribed from RNA using RNA to cDNA EcoDr Premix (TaKaRa). BM cells were collected and washed twice in phosphate buffered saline (PBS), then placed on poly lysine coated slides and allowed to attach. The slides were fixed in 4% (w/v) paraformaldehyde in 1 × PBS for 15 min at room temperature. After fixation, the slides were washed twice in diethy pyrocarbonate (DEPC)-treated PBS (DEPC-PBS) and dehydrated with 70%, 85%, and 99.5% ethanol for 2 min, respectively. Then, cells were permeated for 5 min with 0.5% Triton X-100 in 1 × PBS buffer at 37 °C and followed by washing twice in DEPC-PBS for further reaction.

2.4. The procedure of DCR sensing in vitro

Firstly, cleavage and T4 PNK modification were simultaneously performed in one-step. The reaction mixture contained 1 μM DNAzyme (yield a final concentration of 100 nM in the RCA reaction), various concentrations of RNA substrate, 2 U/μL RNase inhibitor, and 0.5 U/μL T4 PNK in 1 × cleavage buffer (100 mM $MgCl_2$, 10 mM Tris-HCl, 100 mM KCl, 0.01 mg/mL BSA) to yield a final volume of 10.5 μL, then was incubated at 37 °C for 30 min.

Following, the RCA was performed in 1 × phi29 polymerase buffer (50 mM Tris-HCl, 10 mM $(NH_4)_2SO_4$, 10 mM $MgCl_2$, 4 mM DTT, pH 7.5) with addition of 15% deionized formamide, 0.5 U/μL phi29 DNA polymerase, 250 μM dNTPs, 0.2 mg/mL BSA, 200 nM closed circular DNA template and the products of the previous reaction. RCA reaction mixtures with a final volume of 100 μL were incubated at 37 °C for 60 min, and stopped by heating at 90 °C for 5 min. The final resultant products were analyzed by 12% native polyacrylamide gel electrophoresis (PAGE) and the fluorescence spectrum. Note, for the fluorescence spectrum, 1 μM decorator oligos should be simultaneously added in the RCA reaction mixtures. Meanwhile, detection of BCR-ABL1 and ABL1 in the extracted total RNA from CML patients was performed in the same procedure of DCR.

2.5. The procedure of in situ image of BCR-ABL1 mRNA by DCR

The *in situ* image of BCR-ABL1 mRNA in BM cells by DCR was performed as following procedure. To avoid RNA degradation during DCR sensing, all the steps were treated with RNase inhibitor. During the cleavage reaction, the slides were incubated with 2 μM DNAzyme, 2 U/μL RNase inhibitor and 0.5 U/μL T4 PNK in 1 × cleavage buffer (100 mM $MgCl_2$, 10 mM of Tris-HCl, 100 mM of KCl, 0.01 mg/mL BSA) at 37 °C for 1 h. After cleavage, slides were washed by DEPC-treated 2 × SSC with 0.05% tween-20 for 5 min and rinsed in 1 × PBS. Then, RCA was carried out with a mix of 1 × phi29 polymerase buffer, 15% deionized formamide, 0.5 U/μL phi29 polymerase, 0.2 μg/μL BSA, 2 U/μL RNase inhibitor, 500 nM closed circle template, and 250 μM dNTPs. Incubation was kept for 2 h at 37 °C, then washed in 1 × PBS for twice. For detection, slides were incubated with 1 μM decorator oligos in 2 × SSC at 42 °C for 30 min. Then, the non-hybridization oligos were removed by washing twice in 1 × PBS. The dry slides were incubated with 10 μL DAPI and anti-fade mounting medium for 10 min at room temperature to stain the cell nuclei. Images of cells were acquired using an Olympus fluorescence microscope (Olympus, Japan) and a computer-controlled filter wheel with excitation and emission filters for visualization of DAPI, FAM.

3. Results and discussion

3.1. Verification of feasibility of DCR sensing strategy

To evaluate the feasibility of the developed DCR sensing strategy for detection of synthetic BCR-ABL1 RNA *in vitro*, three reactions of DCR were performed in stepwise and the products of each step were analyzed by native PAGE. As shown in Fig. 1A, with introduction of Mg^{2+} into the mixture of the synthetic BCR-ABL1 RNA and DNAzyme, a new band of cleavage fragments with a predicted length could be seen in lane 4 compared to lane 3, proving Mg^{2+} was necessary for DNAzyme catalysis. However, further addition of phi29 polymerase and closed circular DNA template did not result in any amplified products (lane 5), indicating the closed circular DNA template neither react with the primer nor DNAzyme. According to the previous report, DNAzyme-induced cleavage could add a 2′, 3′ cyclic phosphate terminus on the forward-cleaved f1, which blocked the extension of f1 in the presence of phi29 polymerase [38]. Therefore, we treated the cleavage reaction mixture with T4 PNK to remove the terminal 2′, 3′ cyclic phosphate in f1 and then added phi29 polymerase and closed circular DNA template. As shown in lane 6, large fragments of RCA products were appeared with lower mobility and the band of cleavage fragments were disappeared, indicating T4 PNK modification was indispensable for amplifying the cleaved RNA fragments. Meanwhile, along with the increased RCA reaction time, the RCA products were accumulated (lanes 6–8 with reaction time of 15 min, 30 min, 60 min, respectively). Additionally, DCR process was investigated by fluorescence measurement. As shown in Fig. 1B, a strong fluorescence signal was observed after DCR sensing the synthetic BCR-ABL1 RNA, while a low fluorescence signal was obtained in the control reaction without BCR-ABL1 RNA. Thus, the established DCR sensing strategy is capable of sensing BCR-ABL1 RNA *in vitro*.

3.2. Optimization of DCR sensing system

In order to achieve efficient detection performance, several experimental workflows, including one-step, two-step 1 (combine cleavage with T4 PNK reaction in one step), two-step 2 (combine T4 PNK with RCA in one step), and stepwise, were investigated. The highest fluorescence level was obtained in two-step 1, which was similar in the stepwise way (Supporting Information, Fig. S1). Considering the reaction time, we chose the two-step 1 workflow for further application. Mg^{2+} was an important co-factor for DNAzyme catalysis, thus various concentration of Mg^{2+} was introduced into the cleavage reaction. Gradually increased fluorescence intensity was observed with the increasing concentration of Mg^{2+} in the range of 5–80 mM, then the intensity increased slowly (Fig. S2 A). PAGE analysis confirmed the aggregation of cleavage products was correlated with the concentration of Mg^{2+} (Fig. S2B). Consideration of a suitable concentration of Mg^{2+} was strictly for subsequent T4 PNK and RCA reactions, 100 mM of Mg^{2+} was used in DCR sensing system. The influence of the cleavage reaction time was investigated by monitoring the amounts of cleavage products. As shown in Fig. S3 A, the band of cleavage products enhanced along with the reaction time. Also, an increased fluorescence signal along with the increased reaction time and tended to plateau at about 30 min (Fig. S3B). As a result, optimized cleavage time was 30 min. Meanwhile, after analyzing the kinetics curve of DNAzyme cleavage by GraphPad Prism, the k_{obs} (define as the overall rate constant) was calculated to be 0.071 min^{-1}.

3.3. Analytical performance

We investigated the detection sensitivity of DCR sensing strategy to RNA target of BCR-ABL1. The fluorescence signals were gradually increased in response to varying concentrations of BCR-ABL1 (1.0×10^{-15} M to 1.0×10^{-8} M), and a low background signal of DCR sensing system could observe without target (blank) (Fig. 2A). ΔF value, defined as the fluorescence signal difference between with and without the RNA target, was used to quantitatively measure BCR-ABL1 concentration. The ΔF exhibited a linear correlation with the logarithm of BCR-ABL1 concentration in the dynamic range from 10 fM to 10 nM (Fig. 2B). The linear regression equation was $\Delta F = 69.24 \times \lg C_{[BCR\text{-}ABL1]} + 97.31$ ($R^2 = 0.9900$) with the detection limit of 9.4 fM based on 3σ (σ is the standard deviation of the blank). Of note, the achieved LOD was lower than several reported strategies (Table S4). Most RCA-based strategies for amplification of mRNA were depended on the circular DNA templates synthesized in the process of target recognization [22,24]. While, in DCR sensing process, the pre-synthesized circular DNA templates were directly utilized with improved efficiency of the sensing process.

The specificity of DCR was evaluated by determining its response to different RNA sequences. Firstly, BCR-ABL1 and other three interfering RNA samples, including BCR and ABL1 (has partially identical sequences from BCR-ABL1), and BCR-ABL1/S (differs from BCR-ABL1 by single nucleotide) were incubated with DNAzyme for 30 min, respectively. All the interfering RNA samples did not yield distinguishable fluorescence signals from the background, whereas the BCR-ABL1 resulted in an enhanced fluorescence signal (Fig. 2C). PAGE was further applied to evaluate the specificity of the DNAzyme toward different RNA targets. After cleavage products were subjected to electrophoresis, a new band with much faster electrophoretic mobility was observed only in the presence of BCR-ABL1 RNA target (Fig. 2C, inset, lane 4). Meanwhile, there were no obvious cleavage products after DNAzymes reacted with other interfering RNA, validating the specificity of DNAzymes for BCR-ABL1 recognition and cleavage.

Moreover, the analytical recovery was studied by adding different concentrations of BCR-ABL1 in diluted serum (10%) (Table S5). Recoveries of the added BCR-ABL1 were in the range of 92.5% to 108.0%, indicating serum (10%) did not result in significant interference in DCR sensing process. The high accuracy of DCR originates from its intrinsic features, including the precise targeting and cleavage capacity by functional DNAzyme, and the efficient amplification of RCA.

3.4. Detection of BCR-ABL1 mRNA expression in CML patient

For clinical diagnostic of CML, the ratio of BCR-ABL1 to an endogenous control transcript (ABL1 gene) was used to assess the quantity of BCR-ABL1 mRNA. Thus, detection of ABL1 by DCR was constructed as internal reference to quantify the BCR-ABL1 ratio (Supporting Information, Tables S1 - S3, Fig. S4). Based on the DCR strategy, BCR-ABL1 and ABL1 in extracted total RNA samples from 12 CML patients (s1 - s12) were measured first. Then, the BCR-ABL1 ratio of different patients was calculated and compared with the results obtained by commercial RT-PCR kit. As presented in Fig. 3A, there were no significant BCR-ABL1 ratio (s1 - s10) differences between DCR strategy and RT-PCR. While, only two samples with lower BCR-ABL1 mRNA expression (s11 = 2.5%, s12 = 1.3% by RT-PCR) could not be easily detected by DCR. These discrepancies may come from two aspects. First, unlike RT-PCR, DCR sensing strategy directly targets and amplifies the RNA sequences without reverse transcription that may lead the minute difference results on low concentration target. Second, RT-PCR with just one template DNA molecule can yield over 34 billion DNA molecules [39]. While, RCA as an isothermal method typically provides an approximately 1000-fold (for linear amplification) increase

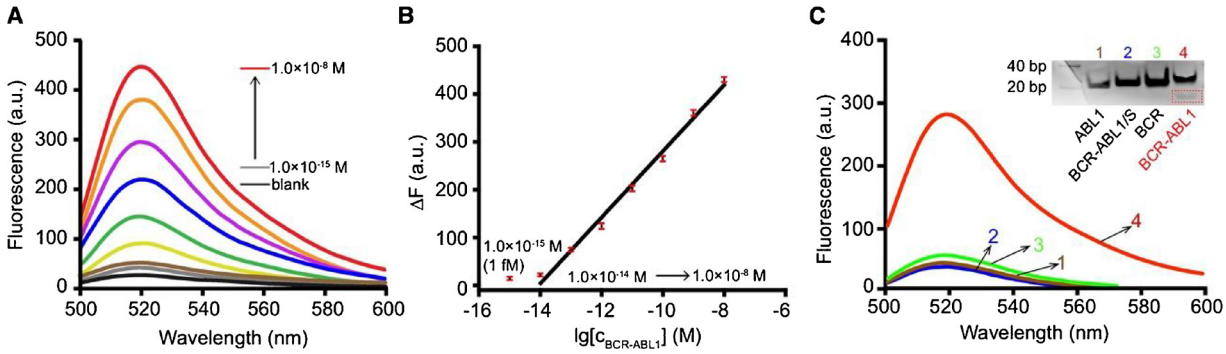

Fig. 2. Sensitivity and specificity of DCR sensing strategy. (A) Fluorescence spectra of DCR strategy in the absence (blank) or presence of BCR-ABL1 with concentrations of 1.0×10^{-15}, 1.0×10^{-14}, 1.0×10^{-13}, 1.0×10^{-12}, 1.0×10^{-11}, 1.0×10^{-10}, 1.0×10^{-9}, and 1.0×10^{-8} M. (B) The linear relationship between ΔF and the logarithm of concentration of BCR-ABL1 in the range of 1.0×10^{-14} to 1.0×10^{-8} M (error bars: SD, n = 3). (C) Fluorescence detection for DCR strategy specificity with BCR-ABL1 (100 pM) and other interfering RNA samples (100 pM). Insets: PAGE of the incubation products of DNAzyme (1 μM) with different RNA samples (500 nM). The cleavage products were shown in the red box(For interpretation of the references to colour in this figure legend, the reader is referred to the web version of this article.).

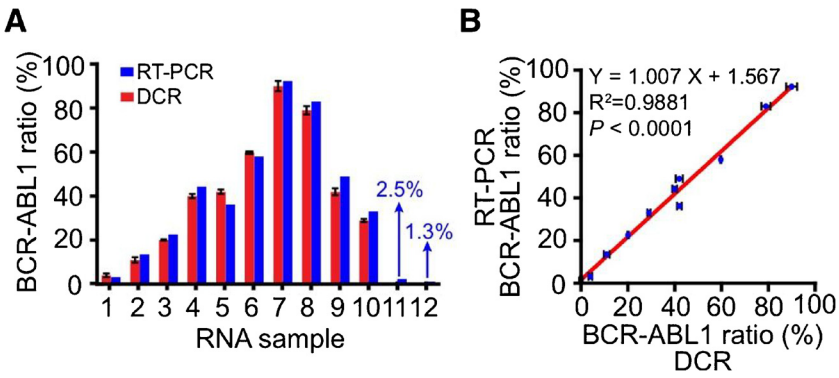

Fig. 3. Detection of BCR-ABL1 mRNA in total RNA sample from 12 CML patients. (A) Histogram and (B) correlation plot showing the BCR-ABL1 ratio of different RNA samples obtained by DCR and RT-PCR (R^2 = 0.9881). Note: The BCR-ABL1 ratio (%) obtained by RT-PCR was a final result for clinical detection without error bars. Error bars: SD, n = 3.

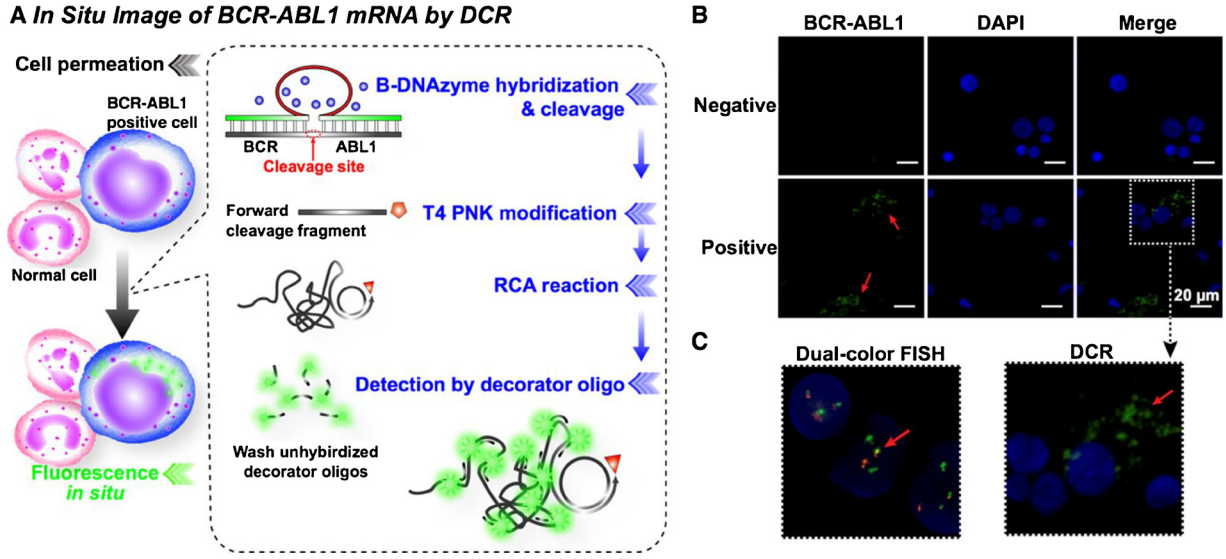

Fig. 4. The feasibility of *in situ* image of BCR-ABL1 mRNA by DCR. (A) A schematic diagram of *in situ* image of BCR-ABL1 mRNA by DCR. (B) Fluorescence images of DCR sensing of BCR-ABL1-positive and BCR-ABL1-negative BM cells. The nuclei in blue by DAPI staining. (C) Fluorescence *in situ* image of BCR-ABL1 mRNA obtained from FISH and DCR. Scale bars = 20 μm(For interpretation of the references to colour in this figure legend, the reader is referred to the web version of this article.).

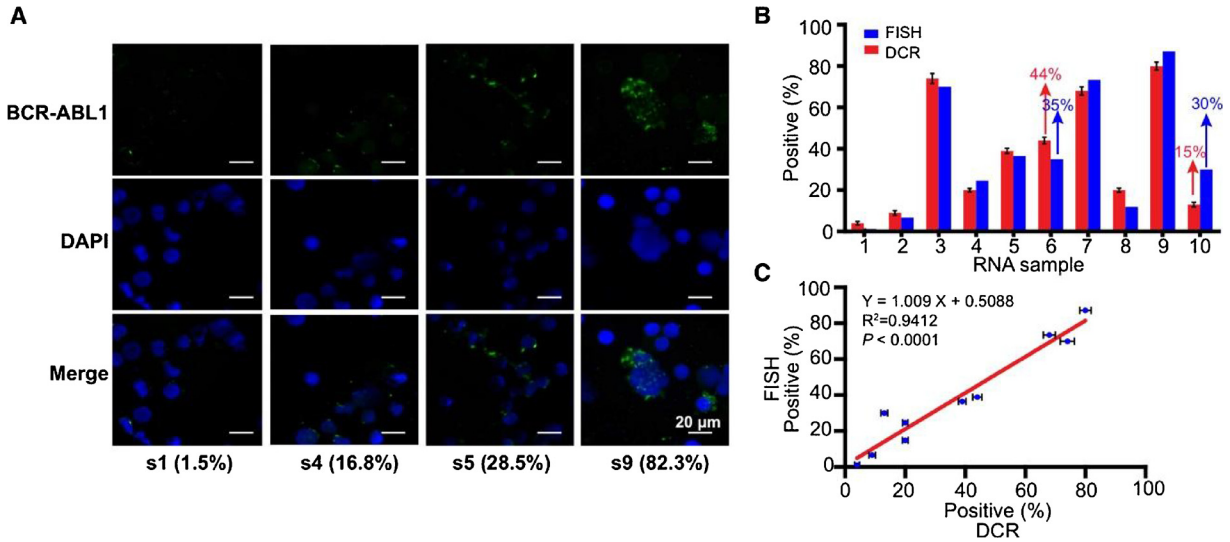

Fig. 5. Detection of BCR-ABL1 mRNA in the cytoplasm of BM cells from CML patients. (A) Imaging of BCR-ABL1 mRNA (green) in the cytoplasm of BM cells. And the BCR-ABL1 ratio measured by RT-PCR of s1, s4, s5 and s9 was 1.5%, 16.8%, 28.5%, and 82.3%, respectively. The nuclei in blue by DAPI staining. Scale bars = 20 μM. (B) Comparison and (C) correlation of percentage of the BCR-ABL1 positive cells between DCR and FISH analysis (n = 10, R^2 = 0.9412). Note: The positive (%) referred to the percentage of BCR-ABL1 positive cells to a total of 200 cells. And the positive (%) obtained by FISH was a final result for clinical detection without error bars. Error bars: SD, n = 3(For interpretation of the references to colour in this figure legend, the reader is referred to the web version of this article.).

in the intensity of the signal [40]. Thus, the detection sensitivity of the two strategies may lead to a difference in the detection of extremely low concentration target. In addition, a linear curve of the BCR-ABL1 ratio obtained by the two strategies was generated to evaluate the correlation between DCR and RT-PCR. As shown in Fig. 3B, the regression equation was $Y = 1.007\ X + 1.567$ with $R^2 = 0.9881$ ($P < 0.0001$), indicating the DCR results were well consistent with the RT-PCR results. Significantly, the DCR strategy has the potential to be a valuable RNA amplification technique because it offers some key advantages that cannot be matched by PCR, such as easy to operation without a thermal cycler equipment, quite simple to design the primer and reported probe, and directly targets and amplifies RNA target. Overall, these results offer the potential application prospects of DCR sensing strategy for the molecular diagnosis of CML in patients.

3.5. *In situ* image of BCR-ABL1 mRNA in bone marrow cells by DCR

The performance of DCR for *in situ* fluorescence image of BCR-ABL1 mRNA was evaluated using the BCR-ABL1 positive or negative bone marrow (BM) cells collected from CML patients (Fig. 4A). The bright, spot-like green signals corresponding to the BCR-ABL1 mRNA were easily distinguished from the background in the positive cells (Fig. 4B). As a control, no discernible fluorescence signal was observed in the negative cells. In clinical diagnosis, dual-color FISH as a conventional cytogenetics technique was considered the "gold standard" for evaluating BCR-ABL1 mRNA *in situ*. As shown in Fig. 4, FISH assay showed only a fuzzy yellow spot (BCR-ABL1) by green (ABL1) and red (BCR) fusion in the BCR-ABL1 positive cell, while abundant green signals for BCR-ABL1 mRNA were obtained after DCR sensing (Fig. 4C). These results suggested that DCR could significantly amplify the detection signal compared to the FISH analysis, originating from the highly efficient RCA amplification. Meanwhile, DCR could successfully perform intracellular imaging of mRNA in living cells.

Finally, we applied our sensing strategy to assay BCR-ABL1 mRNA expression in BM cell from CML patients, ranging from the down expression to over expression. As shown in Fig. 5A, with increasing expression of BCR-ABL1 (results measured by RT-PCR), the green fluorescence signals were brighter in the cells. Moreover, the different expression level of BCR-ABL1 in a single cell could be clearly distinguished on the basis of the fluorescent spots, suggesting DCR could discriminate fluorescence signal among the different mRNA expressions *in situ*. In order to compare the sensitivity of the two methods for their ability to detect BCR-ABL1 mRNA *in situ*, the number of positive cells staining by different methods was counted manually from a total of 200 cells of each BM samples. Of the 10 samples, 8 samples showed good comparability with a difference of 2.3% to 6.5% between DCR *in situ* and FISH through comparison with the percentage of positive (Fig. 5B). While, s6 and s10 with a significant difference of 9% and 15% between the two strategies (Fig. 5B). These differences were attributed to the multistep process and manual counting, which increased the probability of systematic error and induced the minute differences of DCR and FISH. Moreover, the linear relationship between the results in DCR and FISH with a correlation coefficient was 0.9412 and the equation was $Y = 1.009\ X + 0.5088$ ($P < 0.0001$) (Fig. 5C). These results showed no significant difference between the two strategies, suggesting DCR might have potential clinical application for BCR-ABL1 mRNA detection.

4. Conclusions

In summary, an isothermal sensing strategy has been successfully developed for ultrasensitive fluorescence detection and *in situ* image of BCR-ABL1 mRNA by integrating functional DNAzyme with RCA strategy. Resulting from the efficient cleavage of BCR-ABL1 mRNA in a sequence specific manner of DNAzyme, the process of purification and reverse transcription were avoided. Also, the interference of homologous DNA sequences was reduced. Meanwhile, the cleaved-mRNA as a primer in place of an additional DNA primer could reduce the non-specific amplification during the RCA process. Additionally, by adopting RCA, there was no requirement to undergo thermal cyclers to amplify the signals. The developed sensing strategy achieved a highly sensitivity with the detection limit of 9.4 fM for detecting BCR-ABL1. Moreover, this DCR sensing strategy not only specifically detected BCR-ABL1 in extracted RNA samples but also precisely imaged BCR-ABL1 mRNA in BM cells. Therefore, the multifunctional DCR sensing strategy has the potential to analyze RNA targets from the extracellular into intracellular, and also offers new insight into clinical molecular diagnosis and biomedical research.

Acknowledgments

This work was funded by the National Natural Science Foundation of China (81572080), the Special Project for Social Livelihood and Technological Innovation of Chongqing (cstc2016shmszx130043), the Funded Project of Mianyang Municipal Health Bureau (201426) and Funded Project of Third People's Hospital of Mianyang Country (201441).

Appendix A. Supplementary data

Supplementary material related to this article can be found, in the online version, at doi:https://doi.org/10.1016/j.snb.2018.07.032.

References

[1] G.Q. Daley, R.A. Van Etten, D. Baltimore, Induction of chronic myelogenous leukemia in mice by the P210bcr/abl gene of the Philadelphia chromosome, Science 247 (1990) 824–830.
[2] A. Gaiger, T. Lion, P. Kalhs, G. Mitterbauer, T. Henn, O. Haas, et al., Frequent detection of BCR-ABL specific mRNA in patients with chronic myeloid leukemia (CML) following allogeneic and syngeneic bone marrow transplantation (BMT), Leukemia 7 (1993) 1766–1772.
[3] S. Wong, O.N. Witte, The BCR-ABL story: bench to bedside and back, Annu. Rev. Immunol. 22 (2004) 247–306.
[4] S.P. Hunger, CML in blast crisis: more common than we think? Blood 129 (2017) 2713–2714.
[5] J.F. Breininger, D.G. Baskin, Fluorescence in situ hybridization of scarce leptin receptor mRNA using the enzyme-labeled fluorescent substrate method and tyramide signal amplification, J. Histochem. Cytochem. 48 (2000) 1593–1599.
[6] Y. Furukawa, S.L. Ju, H.L. Cho, N. Tatsumi, Detection of bcr-abl fusion mRNA in chronic myelogenous leukemia by reverse transcription polymerase chain reaction using nested primers, Osaka City Med. J. 39 (1993) 35–45.
[7] C. Schrader, A. Schielke, L. Ellerbroek, R. Johne, PCR inhibitors - occurrence, properties and removal, J. Appl. Microbiol. 113 (2012) 1014–1026.
[8] S.A. Bustin, R. Mueller, Real-time reverse transcription PCR and the detection of occult disease in colorectal cancer, Mol. Aspects Med. 27 (2006) 192–223.
[9] D. Li, W. Cheng, Y. Yan, Y. Zhang, Y. Yin, H. Ju, et al., A colorimetric biosensor for detection of attomolar microRNA with a functional nucleic acid-based amplification machine, Talanta 146 (2016) 470–476.
[10] H. Jiang, Y. Xu, L. Dai, X. Liu, D. Kong, Ultrasensitive, label-free detection of T4 ligase and T4 polynucleotide kinase based on target-triggered hyper-branched rolling circle amplification, Sens. Actuators B Chem. 260 (2018) 70–77.
[11] M. Zhang, R. Li, L. Ling, Homogenous assay for protein detection based on proximity DNA hybridization and isothermal circular strand displacement amplification reaction, Anal. Bioanal. Chem. 409 (2017) 4079–4085.
[12] D. Li, W. Cheng, Y. Li, Y. Xu, X. Li, Y. Yin, et al., Catalytic hairpin assembly actuated DNA nanotweezer for logic gate building and sensitive enzyme-free biosensing of microRNAs, Anal. Chem. 88 (2016) 7500–7506.
[13] S.C. Liao, J. Peng, M.G. Mauk, S. Awasthi, J. Song, H. Friedman, et al., Smart cup: a minimally-instrumented, smartphone-based point-of-care molecular diagnostic device, Sens. Actuators B Chem. 229 (2016) 232–238.
[14] Y. Long, X. Zhou, D. Xing, An isothermal and sensitive nucleic acids assay by target sequence recycled rolling circle amplification, Biosens. Bioelectron. 46 (2013) 102–107.
[15] L. Xu, Z. Jiang, Y. Mu, Y. Zhang, Q. Zhan, J. Cui, et al., Colorimetric assay of rare disseminated tumor cells in real sample by aptamer-induced rolling circle amplification on cell surface, Sens. Actuators B Chem. 259 (2018) 596–603.
[16] Y. Liu, F. Luo, B. Wang, H. Li, Y. Xu, X. Liu, et al., STAT3-regulated exosomal miR-21 promotes angiogenesis and is involved in neoplastic processes of transformed human bronchial epithelial cells, Cancer. Lett. 370 (2016) 125–135.
[17] M. Liu, Q. Zhang, D. Chang, J. Gu, J.D. Brennan, Y. Li, A DNAzyme feedback amplification strategy for biosensing, Angew. Chem. Int. Ed. Engl. 56 (2017) 6142–6146.

[18] M. Liu, W. Zhang, Q. Zhang, J.D. Brennan, Y. Li, Biosensing by tandem reactions of structure switching, nucleolytic digestion, and DNA amplification of a DNA assembly, Angew. Chem. Int. Ed. Engl. 54 (2015) 9637–9641.
[19] S. Bi, Y. Cui, L. Li, Ultrasensitive detection of mRNA extracted from cancerous cells achieved by DNA rotaxane-based cross-rolling circle amplification, Analyst 138 (2013) 197–203.
[20] X. Ren, R. Deng, L. Wang, K. Zhang, J. Li, RNA splicing process analysis for identifying antisense oligonucleotide inhibitors with padlock probe-based isothermal amplification, Chem. Sci. 8 (2017) 5692–5698.
[21] R. Deng, L. Tang, Q. Tian, Y. Wang, L. Lin, J. Li, Toehold-initiated rolling circle amplification for visualizing individual microRNAs in situ in single cells, Angew. Chem. Int. Ed. Engl. 53 (2014) 2389–2393.
[22] C.M. Feng, Y. Qiu, E.K. Van Buskirk, E.J. Yang, M. Chen, Light-regulated gene repositioning in Arabidopsis, Nat. Commun. 5 (2014) 3027.
[23] M. Mignardi, A. Mezger, X. Qian, L. La Fleur, J. Botling, C. Larsson, et al., Oligonucleotide gap-fill ligation for mutation detection and sequencing in situ, Nucleic Acids Res. 43 (2015) e151.
[24] R. Deng, K. Zhang, Y. Sun, X. Ren, J. Li, Highly specific imaging of mRNA in single cells by target RNA-initiated rolling circle amplification, Chem. Sci. 8 (2017) 3668–3675.
[25] Z. Wu, H. Fan, N.S.R. Satyavolu, W. Wang, R. Lake, J.H. Jiang, et al., Imaging endogenous metal ions in living cells using a DNAzyme-catalytic hairpin assembly probe, Angew. Chem. Int. Ed. Engl. 56 (2017) 8721–8725.
[26] W. Zhou, Y. Zhang, P.J. Huang, J. Ding, J. Liu, A DNAzyme requiring two different metal ions at two distinct sites, Nucleic Acids Res. 44 (2016) 354–363.
[27] R. Ma, L. Wang, M. Zhang, L. Jia, W. Zhang, L. Shang, et al., A novel one-step triggered "signal-on/off" electrochemical sensing platform for lead based on the dual-signal ratiometric output and electrode-bound dnazyme assembly, Sens. Actuators B Chem. 257 (2018) 678–684.
[28] H. Peng, X.F. Li, H. Zhang, X.C. Le, A microRNA-initiated DNAzyme motor operating in living cells, Nat. Commun. 8 (2017) 14378.
[29] R. Dolot, M. Sobczak, B. Mikolajczyk, B. Nawrot, Synthesis, crystallization and preliminary crystallographic analysis of a 52-nucleotide DNA/2'-OMe-RNA oligomer mimicking 10–23 DNAzyme in the complex with a substrate, Nucleosides Nucleotides Nucleic Acids 36 (2017) 292–301.
[30] D. Zhang, R. Fu, Q. Zhao, H. Rong, H. Wang, Nanoparticles-free fluorescence anisotropy amplification assay for detection of RNA nucleotide-cleaving DNAzyme activity, Anal. Chem. 87 (2015) 4903–4909.
[31] L. Chan, K. Tram, R. Gysbers, J. Gu, Y. Li, Sequence mutation and structural alteration transform a noncatalytic DNA sequence into an efficient RNA-cleaving DNAzyme, J. Mol. Evol. 81 (2015) 245–253.
[32] J.T. Yi, T.T. Chen, J. Huo, X. Chu, Nanoscale zeolitic imidazolate framework-8 for ratiometric fluorescence imaging of microRNA in living cells, Anal. Chem. 89 (2017) 12351–12359.
[33] T.H. Wang, W.T. Li, S.H. Yu, L.C. Au, The use of 10-23 DNAzyme to selectively destroy the allele of mRNA with a unique purine-pyrimidine dinucleotide, Oligonucleotides 18 (2008) 295–299.
[34] D. He, X. He, X. Yang, H.W. Li, A smart ZnO@polydopamine-nucleic acid nanosystem for ultrasensitive live cell mRNA imaging by the target-triggered intracellular self-assembly of active DNAzyme nanostructures, Chem. Sci. 8 (2017) 2832–2840.
[35] S. Lilienthal, M. Klein, R. Orbach, I. Willner, F. Remacle, R.D. Levine, Continuous variables logic via coupled automata using a DNAzyme cascade with feedback, Chem. Sci. 8 (2017) 2161–21618.
[36] J.E. Kim, S. Yoon, B.R. Choi, K.P. Kim, Y.H. Cho, W. Jung, et al., Cleavage of BCR-ABL transcripts at the T315I point mutation by DNAzyme promotes apoptotic cell death in imatinib-resistant BCR-ABL leukemic cells, Leukemia 27 (2013) 1650–1658.
[37] T. Kuwabara, M. Warashina, T. Tanabe, K. Tani, S. Asano, K. Taira, Comparison of the specificities and catalytic activities of hammerhead ribozymes and DNA enzymes with respect to the cleavage of BCR-ABL chimeric L6 (b2a2) mRNA, Nucleic. Acids Res. 25 (1997) 3074–3081.
[38] M. Liu, Q. Zhang, Z. Li, J. Gu, J.D. Brennan, Y. Li, Programming a topologically constrained DNA nanostructure into a sensor, Nat. Commun. 7 (2016) 12074.
[39] D.R. Almassian, L.M. Cockrell, W.M. Nelson, Portable nucleic acid thermocyclers, Chem. Soc. Rev. 42 (2013) 8769–8798.
[40] W. Zhao, M.M. Ali, M.A. Brook, Y. Li, Rolling circle amplification: applications in nanotechnology and biodetection with functional nucleic acids, Angew. Chem. Int. Ed. Engl. 47 (2008) 6330–6337.

Xiao-yan Zhou is currently a Ph. D. of Chongqing Medical University majoring in clinical laboratory diagnosis. Her research interest is the development of biosensing strategy for clinical diagnosis.

Jian-hua Pan is currently a Ph. D. of Chongqing Medical University majoring in clinical laboratory diagnosis. His research interest is the development of biosensing strategy for clinical diagnosis.

Yong-neng Ma is currently a professor of Third People's Hospital of Mianyang country. His research interest is in clinical molecular diagnosis.

Xiu-juan Peng is currently a professor of Third People's Hospital of Mianyang country. Her research interest is in clinical molecular diagnosis.

Hai-ping Wu is currently a master student of Chongqing Medical University majoring in clinical laboratory diagnosis. His research interest is the development of biosensing strategy for clinical diagnosis.

Qin Zhou is currently a professor of Chongqing Medical University majoring in clinical laboratory diagnosis. His research interest is the development of biosensing strategy for clinical laboratory diagnosis.

Shi-jia Ding is currently a professor of Chongqing Medical University majoring in clinical laboratory diagnosis. His research interest is the development of biosensing strategy for clinical laboratory diagnosis.

Huang-xian Ju is a Changjiang Scholar Professor of chemistry, and Director of Key Laboratory of Analytical Chemistry for Life Science (Ministry of Education of China) in Nanjing University. His research interests are in bioanalytical chemistry, molecular diagnosis, biosensors and clinic immunoassay.